

Reducing rotor speed variations of floating wind turbines by compensation of non-minimum phase zeros

Boris Fischer,

Fraunhofer Institute for Wind Energy and Energy System Technology (IWES), Division Control Engineering and Energy Storages, Email: boris.fischer@iwes.fraunhofer.de

Abstract:

Applying a land-based designed pitch controller on a floating wind turbine may cause severe instability. A common strategy to overcome this problem is to reduce the closed-loop bandwidth of the pitch control system. In so doing, the generator speed variation increases possibly leading to shutdowns due to overspeeds. This study uses a parallel path modification to avoid instability without increasing the generator speed variation. The results of comprehensive simulations and load calculations carried out on the 5MW NREL offshore wind turbine installed on the OC3-Hywind spar buoy are presented. These demonstrate that by using the proposed method it is possible to apply the land-based designed pitch controller on its floater-based equivalent.

Keywords: floating wind turbine, control system, parallel path modification.

1 Introduction

Many works on the control of floating wind turbines point out the issue of negative damping of the platform pitch motion because of interactions between the blade-pitch control system and tower motions, e.g. [1, 2, 3]. From a control engineering point of view, this is due to a complex pair of non-minimum phase zeros (NMPZ) of the transfer function from the blade-pitch angle to the generator speed.

These zeros also occur on land-based wind turbines and they are a hard limit for the bandwidth of the blade-pitch controller [4]. While they are located near the natural frequency of the first tower bending mode for fixed turbines, they are located near the natural frequency of the platform pitch mode for floating turbines. Unfortunately, the platform pitch frequency is quite low, because it has to lie well below the peak of the wave spectrum to avoid the excitation of heavy loads on the structure [2].

It is a straightforward approach to reduce the closed-loop bandwidth of the blade-pitch control system below the platform pitch frequency

[1, 2]. But the reduced bandwidth causes the generator speed to respond more sensitive to disturbances. Reference [2] reports that for the floating system with reduced bandwidth the maximum rotational speed is up to 30% higher than the nominal speed, whereas typical values for onshore turbines are up to 10%. These values are confirmed by the simulation results given below. The increased variations are especially critical for wind turbines with doubly fed induction generators, which are usually designed with a variable speed range of $\pm 30\%$ around the synchronous speed [5].

The restrictions induced by the NMPZ can be overcome. This is shown in [4] for fixed-foundation turbines. In this paper, it is demonstrated how the method can be applied to reduce the rotor speed variations of floating wind turbines.

In the next section, linear control design models are presented that feature the relevant dynamic properties. The subsequent section summarises the results of a simulation study where the method is applied to a widely-used benchmark system: the 5MW NREL offshore wind turbine installed on the OC3-Hywind spar buoy [6]. All simulations have been carried out in Matlab/Simulink with the FAST module [7], a fully coupled aero-hydro-servo-elastic code, which is freely available and has been developed at the National Renewable Energy Laboratory.

2 Control method

After introducing a very simple model to analyse the emergence of the NMPZ, the approach to compensate them is presented. For the latter purpose, a more complex linear model is used.

2.1 Analysis and control design models

A very simple, 1.5 DOF model, linearised around a certain operating point, is sufficient to investigate where the NMPZ come from. Therefore, all the time varying physical quanti-

ties in the formulas below are defined as deviations from their steady state values.

The model consists of a second order differential equation for the platform pitch mode

$$J_T \ddot{\varphi} + D_T \dot{\varphi} + C_T \varphi = L_T F_{th},$$

where φ is the platform pitch angle and F_{th} is the thrust force on the nacelle, see Figure 1. As the wave excitation is an external disturbance for the control loop it has been neglected for the following stability considerations. The rotating parts are summarised using a first order differential equation

$$J_R \dot{\omega} = T_{aero} - T_{gen},$$

where ω is the rotational speed, and T_{aero} and T_{gen} are the aerodynamic and the generator torque, respectively. Furthermore, the aerodynamics are approximated by the gradients of the rotor characteristics:

$$\begin{aligned} F_{th} &= c_{F,v}(v_w - L_T \dot{\varphi}) + c_{F,\omega} \omega + c_{F,\beta} \beta \\ T_{aero} &= c_{T,v}(v_w - L_T \dot{\varphi}) + c_{T,\omega} \omega + c_{T,\beta} \beta, \end{aligned}$$

where the constants $c_{F,v}$ and $c_{T,v}$ are the gradients of thrust force and aerodynamic torque with respect to the effective, local wind speed at the blades – valid in the vicinity of the operating point. The other constants are the gradients with respect to rotor speed ω and blade pitch angle β .

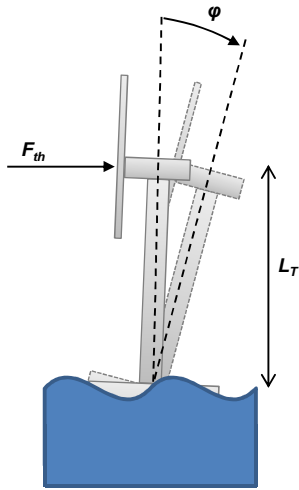


Figure 1: Schematic for the equation of the platform pitch mode.

For the design of the pitch controller we need the transfer function from the blade pitch angle to the rotor speed. It is obtained by using Laplace transformed versions of the equations above:

$$\omega(s) = \frac{\frac{C_T}{J_T} + \frac{1}{J_T} (D_T + \mu_{aero} L_T^2) s + s^2}{a_0 + a_1 s + a_2 s^2 + a_3 s^3} \beta(s),$$

with the abbreviation

$$\mu_{aero} = c_{F,v} - c_{T,v} \frac{c_{F,\beta}}{c_{T,\beta}}$$

in the numerator, and the coefficients a_i of the denominator polynomial.

Now it can be seen that the transfer function exhibits a pair of NMPZ if

$$\mu_{aero} L_T^2 < -D_T,$$

that is, the occurrence of the NMPZ depends on the ratio of the aerodynamic coefficients μ_{aero} and the damping of the platform pitch mode D_T .

The coefficient μ_{aero} varies with the operating point and is usually very low near rated wind speed. It also provides an insight into the underlying physics: $c_{F,v}$ and $c_{T,v}$ are both positive, $c_{F,\beta}$ and $c_{T,\beta}$ are both negative for power production operating points. Hence, there are two physical pathways (via thrust force and via aerodynamic torque) with different signs, which is a necessary condition for the emergence of NMPZ.

Although the simple, 1.5 DOF model is sufficient for the explanation of the NMPZ a more complex linear model is necessary for the overall control design. To this end, the model introduced in [8] has been enhanced by the relevant hydrodynamic effects.

Figure 2 exemplarily shows the non-minimum phase behaviour of this model. The blue dotted line is the phase response from blade-pitch angle to generator speed of the model with the operating point at 13 m/s constant wind speed. Between 0.2 and 0.3 rad/s, which is the frequency range in which the natural frequency of the platform pitch motion is located, the phase loss due to the NMPZ is clearly present.

Two other modes can be taken from the phase plot: first, the platform surge mode around 0.05 rad/s, which does usually not cause non-minimum phase behaviour, as it is damped enough, and second, the first tower bending mode in fore-aft direction around 3 rad/s, which usually is the origin of the non-minimum phase behaviour of land-based wind turbines.

The linear model is validated in the critical frequency range with a manual, pointwise open loop “measurement” of the transfer function using the non-linear simulation code FAST [7] (red marks). For that purpose, the simulation model has been driven to the steady operating point at 13 m/s constant wind speed and still water. Then the controller has been switched off and the collective blade pitch has been

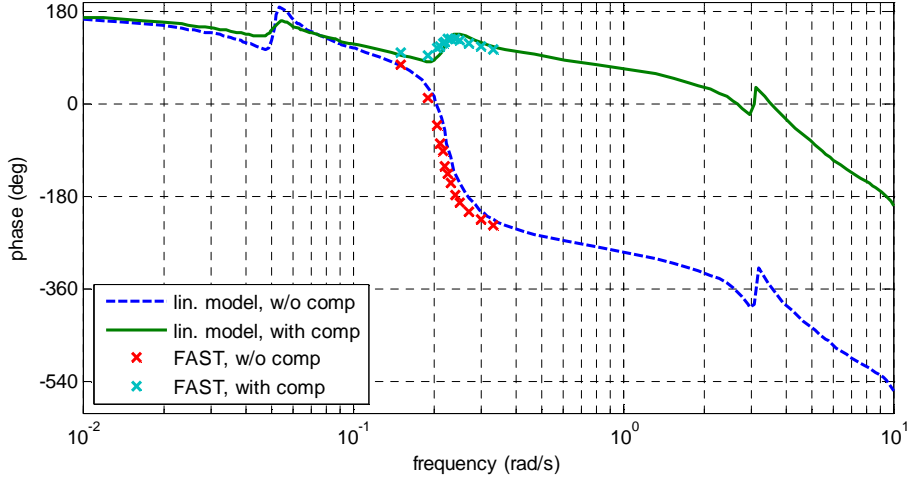


Figure 2: Phase response from collective pitch angle to generator speed with and without NMPZ compensation. Comparison of a linear model along the lines of [8] and a manual, pointwise “measurement” using the non-linear simulation code FAST [7].

modulated with harmonic oscillations of different frequencies.¹

2.2 NMPZ compensation

As mentioned in the introduction, this complex pair of NMPZ is a hard constraint for the control design. For the example, the closed-loop bandwidth of a conventionally designed blade-pitch control system will be below 0.2 rad/s, which is an order of magnitude lower than for a common multi-megawatt onshore wind turbine.

Theoretically, the non-minimum phase effect could be avoided by an appropriate design of the aerodynamic properties of the rotor (μ_{aero}) or the hydrodynamic properties of the floating platform (D_T). Whether such designs are feasible in practice is beyond the scope of this paper. It is focussed on a modification of the control system of the wind turbine to overcome the bandwidth problem.

In [4] it is shown how the constraints induced by the NMPZ can be overcome for a fixed-foundation wind turbine by a technique called parallel path modification, see [9]. The general idea is to compensate the NMPZ between one input and one output of the plant by using a second input and a second output.

For the wind turbine the latter two are the generator torque and nacelle velocity in fore-aft direction, see Figure 3. That is, by feeding back the nacelle velocity to the generator

torque it is possible to modify the zeros of the transfer function from blade-pitch to generator speed. The same approach is obviously suitable for floating wind turbines.

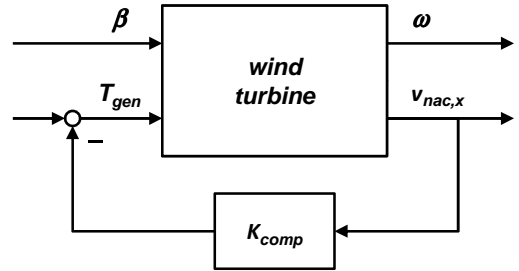


Figure 3: Block schematic of the parallel path modification. The NMPZ of the transfer function from blade pitch β to generator speed ω is compensated by feeding back the nacelle velocity $v_{nac,x}$ to the generator torque T_{gen} .

A proportional feedback of the nacelle velocity $v_{nac,x} = L_T \cdot \dot{\phi}$ to the generator torque, i.e.

$$T_{gen} = -K_{comp} L_T \dot{\phi},$$

leads to a modified aerodynamic coefficient

$$\tilde{\mu}_{aero} = c_{F,v} - (c_{T,v} - K_{comp}) \frac{c_{F,\beta}}{c_{T,\beta}}.$$

Clearly, the proportional feedback can be used to adjust the coefficient arbitrarily.

Figure 2 demonstrates this for the example system from the last section and $K_{comp} = 0.5 c_{T,v}$. The NMPZ close to the frequency of the platform pitch is compensated and the dramatic phase loss has vanished, for the complex linear model (green line) as well as for the manual measurement using the nonlinear

¹ FAST, which has also been used for the simulation study below, features a linearization capability. Although the linearisation routine properly identifies the magnitude response, the corresponding phase response does not show the non-minimum phase behaviour that is “measured” manually.

model (turquoise marks). This enables the control designer to choose an increased bandwidth for the rotor speed closed loop, which, in turn, reduces rotor speed variations and the risk of overspeeds.

It can be argued that using additional inputs and outputs allows for the application of multi-variate control design methods, see e.g. [10]. These methods intrinsically include the opportunity to compensate the said non-minimum phase behaviour. However, to the best of the author's knowledge, these advanced control concepts have not yet been widely applied in the wind industry besides some example research projects, see also the discussion on this topic in [11]. Common practice in industry is to iteratively close several more or less decoupled SISO control loops, each of which is dedicated to different tasks (rotor speed regulation, drive train damper, etc.). The proposed method is in accordance with this approach.

As the loads on the wind turbine are particularly influenced by the control system, the application of the NMPZ compensation in practice has to be carefully balanced, especially with respect to the drive train loads. Therefore, the results of a simulation study are presented in the next section. Another important implementation aspect is that the readily available sensor signal is the nacelle fore-aft acceleration. That is, filtering is also necessary to a certain extent.

3 Simulation study

The method is exemplarily applied to the 5MW NREL offshore wind turbine installed on the OC3-Hywind spar buoy [6]. All simulations have been carried out in Matlab/Simulink with the FAST module [7].

3.1 Simulation set-up

To demonstrate the recovered bandwidth, the blade-pitch controller originally designed for the land-based version [12] is applied to the OC3-Hywind version [6], what is apparently

impossible without using the compensator [1]. Although this approach is a little academic – from a practical point of view it would make sense to redesign the blade-pitch controller for the wind turbine including the compensator – it is very useful for demonstrating the effects of the NMPZ compensation. For comparison, the original wind turbines with unmodified control systems are also considered: the land-based turbine from [12] and the floating system from [6]. All three configurations are summarized in the Table 1.

A fatigue load analysis has been carried out in accordance with DLC1.2 of the IEC 61400-3 standard (normal operation). The different simulated environmental conditions are:

- 4, 6, 8, ..., 24 m/s mean wind speeds (IEC I, B; power law exponent 0.14), no yaw misalignment, and
- site-specific metocean data according to [13], a location in the northern North Sea.

Each simulation run takes 850 seconds, while the first 250s are omitted for the analysis to exclude transients due to initialization effects. 5 different random seeds are used for each wind speed, i.e. the total number of simulation runs with all three turbine configurations is 165.

3.2 Analysis

Figure 4 shows sample time series of the floating configurations for a simulation run with 14 m/s mean wind speed. It demonstrates qualitatively the main differences between the system with and without the NMPZ compensator, i.e. configuration C and B, respectively.

The intended purpose of the NMPZ compensator is clearly to be seen: generator speed variations are greatly reduced for configuration C. This improvement is due to the increased bandwidth of the blade-pitch control loop, as indicated by the faster blade-pitch action. Furthermore, while for configuration B the generator torque is held constant in the region above

Table 1: Three configurations have been simulated for the load calculations.

<i>configuration</i>	<i>platform</i>	<i>blade-pitch controller</i>	<i>generator-torque controller</i>
A	land-based	high bandwidth (according to [12])	constant power (according to [12])
B	OC3-Hywind spar buoy	low bandwidth (according to [6])	constant torque (according to [6])
C	OC3-Hywind spar buoy	high bandwidth (according to [12])	constant torque (according to [6]) + NMPZ compensator

rated wind speed, the NMPZ compensator uses the generator torque dynamically.

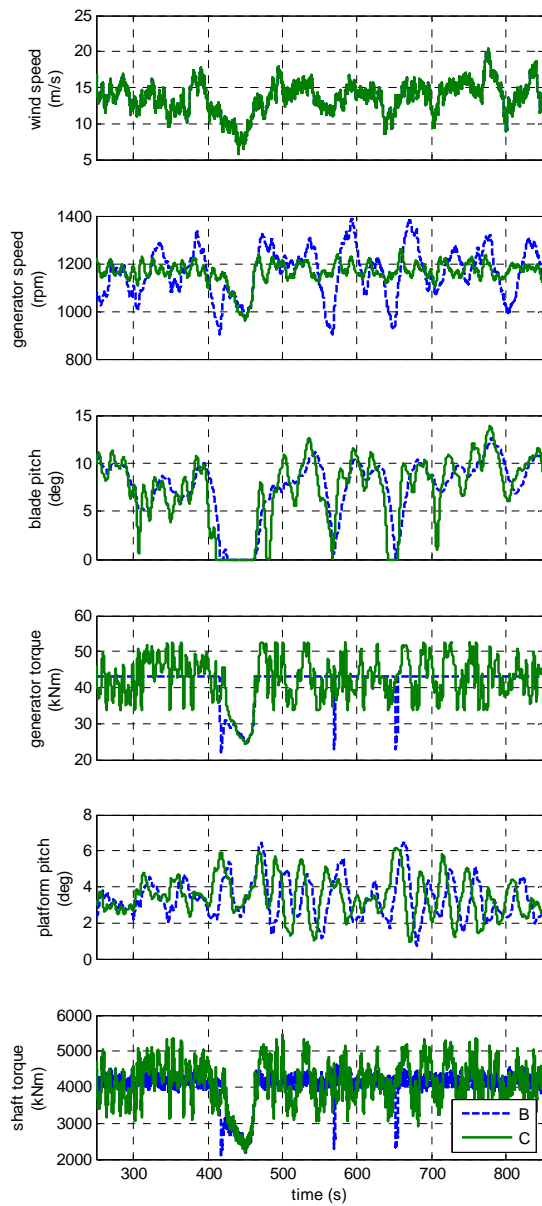


Figure 4: Time series of the floating configurations for a simulation run with 14 m/s mean wind speed. B: Low bandwidth blade-pitch controller. C: High bandwidth blade-pitch controller and NMPZ compensator.

A saturation element has been applied to limit the generator torque used by the compensator around $\pm 20\%$ of the nominal generator torque. This avoids too high generator torque demands. To this end, the generator torque maximum has been increased to 120% of its nominal value, in contrast to [6] and [12], where the maximum value is assumed to be 110%.

Both configurations are similar with respect to the platform pitch motion. This is of course not the case for the shaft torque. The increased

usage of the generator torque leads to heavier fluctuations drive train torque.

Those qualitative findings are now quantified with a statistical analysis and a load calculation taking into account all the simulation runs.

Figure 5 shows the statistics of the generator speed with respect to the mean wind speed of the simulation run. For each wind speed there are 5 simulation runs. The generator speed variations of land-based turbine and the floating turbine with NMPZ compensator are similar ($\pm 10\%$) around nominal in the region above rated). For the floating turbine with slow blade-pitch controller the maximum overspeed is about 30% of the nominal value – as observed in [2].

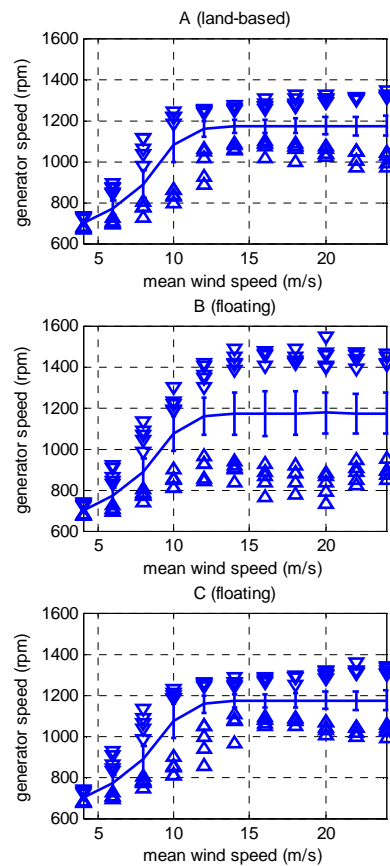


Figure 5: Maximum, minimum, mean and standard deviation of the generator speed vs. mean wind speed.

In the same manner, Figure 6 summarises the statistics of the platform pitch angle for the floating turbines. The platform pitch angle variation is comparable for both configurations, except for an outlier at 14m/s wind speed in configuration C.

Finally, fatigue load calculations have been performed for each turbine configuration. The resulting damage equivalent loads (DELs) of

the floating turbines are divided by the DELs of the land-based turbine. Thus, a DEL ratio of 1.05 means that the corresponding DEL of the floating system is increased by 5% with respect to the land-based system.

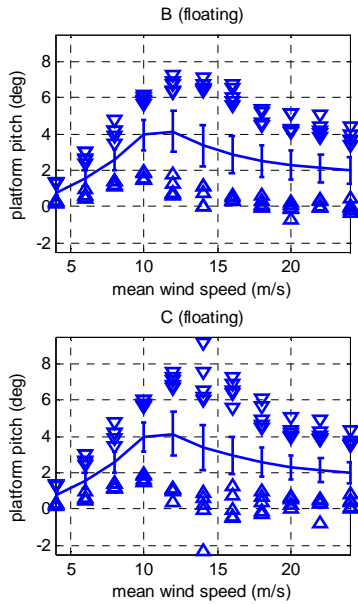


Figure 6: Maximum, minimum, mean and standard deviation of the platform pitch angle vs. mean wind speed.

The DEL ratios of the main shaft torsion are shown in Figure 7, the blade-root bending moments and the tower-base bending moments. These are obtained by a cumulative rainflow count weighted by a Weibull distribution. A Wöhler exponent $m=10$ has been used for the blade related quantities, for all other quantities $m=4$.

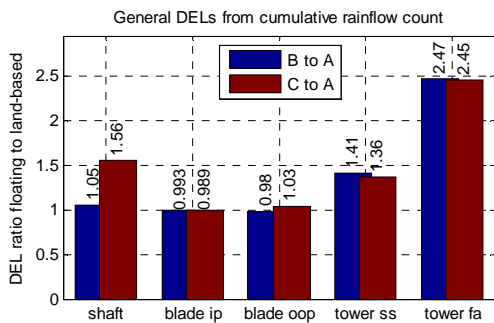


Figure 7: General DEL ratios from rainflow count. The values of the floating turbines are divided by the land-based turbine.

Configuration B has been investigated in [14], too, and the DEL ratios reported there coincide with those in Figure 7: While the tower-base bending moments are increased, the other values are similar. The same holds true for the floating system with compensator (configuration C) except for the main shaft torsion. Unsurprisingly, because the RHPZ compensator uses the generator torque, these loads are

increased by 56% compared to the land-based system.

The DEL obtained by a rainflow cycle count is a good measure for the torsional fatigue of the main shaft. In case of components like the gearbox and the main bearings, the DELs obtained by calculating the load duration distribution is more meaningful [15]. These drive train DEL ratios are shown in Figure 8. There is no significant difference between the two floating configurations.

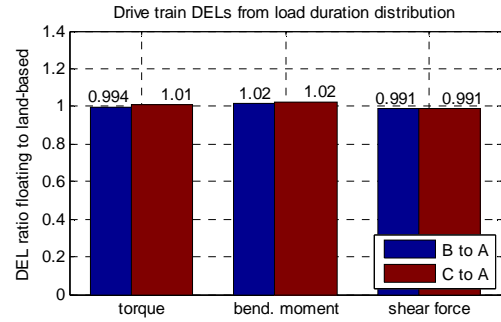


Figure 8: DEL ratios of the drive train from load duration distribution. The values of the floating turbines are divided by the land-based turbine.

The fatigue load calculations show only one significant difference between the two floating configurations. The use of the generator torque for the RHPZ compensator increases the torsional fatigue of the main shaft. Whether this is suitable for the wind turbine cannot be said in general as this depends on the specific components of the wind turbine design.

4 Conclusion

The method introduced in [4] for fixed foundation wind turbines can also be applied to floating wind turbines to successfully reduce rotor speed variations. Compensation of a complex pair of NMPZ renders it possible to increase the bandwidth of the blade-pitch control loop of the floating wind turbine. The achievable bandwidth is similar to that of the corresponding land-based system.

The simulation study demonstrates that it is even possible to apply the land-based designed pitch controller on its floater-based equivalent. It has also been indicated that the fatigue loads experienced by the floating wind turbine with NMPZ compensator remain constant in comparison to the same floating system without the compensator – except for the main shaft torsion DEL obtained by rainflow count, which is increased by a factor of 1.5. On the other hand, the maximum overspeed in the simulations is decreased from 30% to 10% of the rated value.

Acknowledgement

This work has been carried out in the framework of the 7th Framework Integrated Project "HiPRwind", co-funded by the European Community.

References

- [1] Jonkman J. "Influence of control on the pitch damping of a floating wind turbine", in: 46th AIAA aerospace science meeting and exhibit, Reno, Nevada; 2008.
- [2] Larsen T, Hanson T. "A method to avoid negative damped low frequent tower vibrations for a floating, pitch controlled wind turbine", in: The science of making torque from wind. J Phys: Conf Ser, vol. 75. DTU, Copenhagen (DK); 2007.
- [3] Skaare B, Hanson T, Nielsen F, Yttervik R, Hansen A, Thomsen K, Larsen T. "Integrated dynamic analysis of floating offshore wind turbines", in: Proceedings of the EWEC 2007, Milan, Italy; 2007.
- [4] Leithead W, Dominguez S. "Coordinated Control Design for Wind Turbine Control Systems", In: Scientific proceedings of the EWEC 2006, Athens, Greece, pp. 56-59.
- [5] Li H, Chen Z. "Overview of different wind generator systems and their comparisons", IET Renew. Power Gener., 2008, Vol. 2, No. 2, pp. 123–138.
- [6] Jonkman J. "Definition of the Floating System for Phase IV of OC3", NREL/TP-500-47535, technical report, May 2010.
- [7] Jonkman J, Buhl M. "FAST User's Guide", NREL/EL-500-38230, technical report, August 2005.
- [8] Jasiewicz B, Geyler M. "Wind turbine modelling and identification for control system applications", in: Scientific proceedings of the EWEA 2010, Bruxelles, Belgium, pp. 280-283.
- [9] Horowitz I. "Synthesis of Feedback Systems", Academic Press, 1963.
- [10] Namik H, Stol K. "Disturbance Accomodating Control of Floating Offshore Wind Turbines", 47th AIAA Aerospace Sciences Meeting, January 2009.
- [11] Bossanyi E A, Ramtharan G, Savini B. "The Importance of Control in Wind Turbine Design and Loading", 17th Mediterranean Conference on Control and Automation, pp.1269-1274, 2009.
- [12] Jonkman J, Butterfield S, Musial W, Scott G. "Definition of a 5-MW Reference Wind Turbine for Offshore System Development", NREL/TP-500-38060, technical report, February 2009.
- [13] Jonkman J. "Dynamics Modeling and Loads Analysis of an Offshore Floating Wind Turbine", NREL/TP-500-41958, November 2007.
- [14] Jonkman J, Matha D. "Dynamics of offshore floating wind turbines – analysis of three concepts", Wind Energy, 2011, 14, pp. 557-569.
- [15] Niederstucke B., Anders A, Dalhoff P, Grzybowski R. "Load data analysis for wind turbine gearboxes", Technical report, Germanischer Lloyd WindEnergie GmbH, 2002.